Ste20-Related Proline/Alanine-Rich Kinase (SPAK) Regulated Transcriptionally by Hyperosmolarity Is Involved in Intestinal Barrier Function

Yutao Yan, Guillaume Dalmasso, Hang Thi Thu Nguyen, Tracy S Obertone, Shanthi V Sitaraman, Didier Merlin

OPEN ACCESS Freely available online

PLoS one

Ste20-Related Proline/Alanine-Rich Kinase (SPAK) Regulated Transcriptionally by Hyperosmolarity Is Involved in Intestinal Barrier Function

Yutao Yan*, Guillaume Dalmasso, Hang Thi Thu Nguyen, Tracy S. Obertone, Shanthi V. Sitaraman, Didier Merlin

Department of Medicine, Division of Digestive Diseases, Emory University School of Medicine, Atlanta, Georgia, United States of America

Abstract

The Ste20-related protein proline/alanine-rich kinase (SPAK) plays important roles in cellular functions such as cell differentiation and regulation of chloride transport, but its roles in pathogenesis of intestinal inflammation remain largely unknown. Here we report significantly increased SPAK expression levels in hyperosmotic environments, such as mucosal biopsy samples from patients with Crohn's disease, as well as colon tissues of C57BL/6 mice and Caco2-BBE cells treated with hyperosmotic medium. NF-κB and Sp1-binding sites in the SPAK TATA-less promoter are essential for SPAK mRNA transcription. Hyperosmolarity increases the ability of NF-κB and Sp1 to bind to their binding sites. Knock-down of either NF-κB or Sp1 by siRNA reduces the hyperosmolarity-induced SPAK expression levels. Furthermore, expression of NF-κB, but not Sp1, was upregulated by hyperosmolarity *in vivo* and *in vitro*. Nuclear run-on assays showed that hyperosmolarity increases SPAK expression levels at the transcriptional level, without affecting SPAK mRNA stability. Knockdown of SPAK expression by siRNA or overexpression of SPAK in cells and transgenic mice shows that SPAK is involved in intestinal permeability *in vitro* and *in vivo*. Together, our data suggest that SPAK, the transcription of which is regulated by hyperosmolarity, plays an important role in epithelial barrier function.

Citation: Yan Y, Dalmasso G, Nguyen HTT, Obertone TS, Sitaraman SV, et al. (2009) Ste20-Related Proline/Alanine-Rich Kinase (SPAK) Regulated Transcriptionally by Hyperosmolarity Is Involved in Intestinal Barrier Function. PLoS ONE 4(4): e5049. doi:10.1371/journal.pone.0005049

Editor: Stefan Bereswill, Charité-Universitätsmedizin Berlin, Germany

Received February 2, 2009; **Accepted** February 6, 2009; **Published** April 3, 2009

Funding: This work was supported by National Institutes of Health of Diabetes and Digestive and Kidney Diseases by grants R24-DK-064399 (center grant), RO1-DK-061941 (to D. Merlin), RO1-DK55850 (S. Sitaraman). Y. Yan is a recipient of a research fellowship award from the Crohn's and Colitis Foundation of America. The funders had no role in study design, data collection and analysis, decision to publish, or preparation of the manuscript.

Competing Interests: The authors have declared that no competing interests exist.

* E-mail: yyan2@emory.edu

Introduction

Inflammatory bowel diseases (IBD), including ulcerative colitis (UC) and Crohn's disease (CD), are multi-factorial diseases typically associated with relapsing diarrhea, which is caused by increased paracellular permeability of the intestinal epithelial lining and an intestinal hyperosmotic environment [1,2,3,4,5]. Intestinal epithelial cells (IECs) are exposed to the second most extreme osmotic environment after kidney. In many forms of IBD, including CD, neonatal necrotizing enterocolitis and UC, this extreme hyperosmolarity contributes to the exacerbation of intestinal inflammation via upregulation of inflammatory molecules such as matrix metalloproteinase (MMP)-9 [6], epithelial cytokine response-interleukin (IL)-8 [7,8,9,10], IL-1 [11,12,13], and tumor necrosis factor (TNF)-α [13], downregulation of vascular cell adhesion molecule (VCAM)-1 [14], or methylation of protein phosphatase 2A [15]. Thus, hyperosmolarity is recognized as a proinflammatory signal [12,16] in addition to classic inflammatory signals including bacteria, bacterial byproducts or proinflammatory cytokines. In addition to IECs, osmotic stress presents an important challenge to normal cell function in a variety of other cells, including peripheral blood mononuclear cells [7], human bronchial epithelial cells [8,9] and the corneal epithelium [17]. Hyperosmolarity has been proposed to play a role in intestinal inflammation in several inflammatory bowel diseases, including CD and UC, as well as newborn and neonatal necrotizing enterocolitis [1,2,3,4,5].

Yeast ste20 kinases, and the mammalian homologs p21-activated kinase (PAK) and germinal center kinase (GCK), function as mitogen-activated protein kinase kinase kinase kinases (MAP4K) and have central and well-described roles in "cell-volume sensing" and in regulating a wide variety of gene functions, including barrier-related functions [18,19,20,21,22]. Lymphocyte-oriented kinase (LOK, ste20-like kinase) [23] and Ste20-like kinase (SLK) [24] can regulate actin cytoskeleton reorganization during cell adhesion and spreading, whereas PAK increases endothelial permeability [25,26].

The ste20-like proline/alanine-rich kinase (SPAK) belongs to the GCK IV subfamily, members of which contain an N-terminal series of proline and alanine repeats (PAPA box), followed by a catalytic domain, a nuclear localization signal, a consensus caspase-cleavage motif, and a C-terminal regulatory region [27], with the missing PAPA box and F-alpha helix loop present in its colonic isoform [28,29]. SPAK plays roles in cell differentiation [27,30], cell transformation and proliferation [31], regulation of chloride transport [32,33,34], and mediation of intestinal

inflammation [29]. Specifically, SPAK can phosphorylate Na^+-K^+-$2Cl^-$ cotransporter 1 (NKCC1), which has an important role in inflammation [35,36] and maintaining intracellular and extracellular ion homeostasis [37]. Recently, we have demonstrated that under inflammatory conditions, TNF-α is a key regulator of SPAK expression [29].

The relationships among hyperosmolarity, SPAK and IBD are unknown. A better knowledge of these relationships will further our understanding of IBD physiopathology. The present study was therefore undertaken to determine how SPAK expression is regulated by hyperosmolarity and investigate its involvement in epithelial barrier function loss, which occurs during IBD.

Results

Colonic SPAK is upregulated in patients with CD

As a preliminary step in a functional study of SPAK in IBD, it is sensible to study its expression profile. We examined SPAK expression in colonic biopsy samples from healthy and CD patients. Immunofluorescence of biopsy specimens from CD patients showed increased colonic SPAK expression, mainly in epithelial cells, compared with specimens of healthy colon tissue (Fig. 1A). Real-time PCR and Western-blot analyses showed that colonic mucosa from the same CD patients contained significantly increased SPAK expression at both the mRNA and protein levels compared with tissue from normal subjects (Fig. 1B and 1C).

Expression of SPAK is enhanced in colon tissue from hyperosmolarity treated mice

Next we examined the relative SPAK expression levels in colon samples from healthy mice and mice exposed to hyperosmotic conditions. Immunofluorescence analysis showed increased levels of colonic SPAK expression, mainly in epithelial cells, compared with sections from untreated colonic tissue (Fig. 2A). As shown in Fig. 1A and 2A, hyperosmolarity induces cell-wall damage and tissue shrinkage, and increases the space between crypts. Epithelial damage is apparent as early as 1 day after exposure to hyperosmolarity and progressively increases to a maximum level at day 5. Correspondingly, SPAK mRNA (Fig. 2B) and protein (Fig. 2C) levels in colonic tissue increase under hyperosmotic conditions and correlate with the extent and duration of colonic injury (Fig. 2A). The greatest increases in SPAK expression levels were on days 3 and 5; SPAK transcripts were detected at approximately 2.7-fold greater levels compared with untreated mice (Fig. 2B), as shown by real-time PCR, immunohistochemistry and Western-blot analyses. Together, these results indicate a strong correlation between SPAK expression level and the extent of hyperosmolarity.

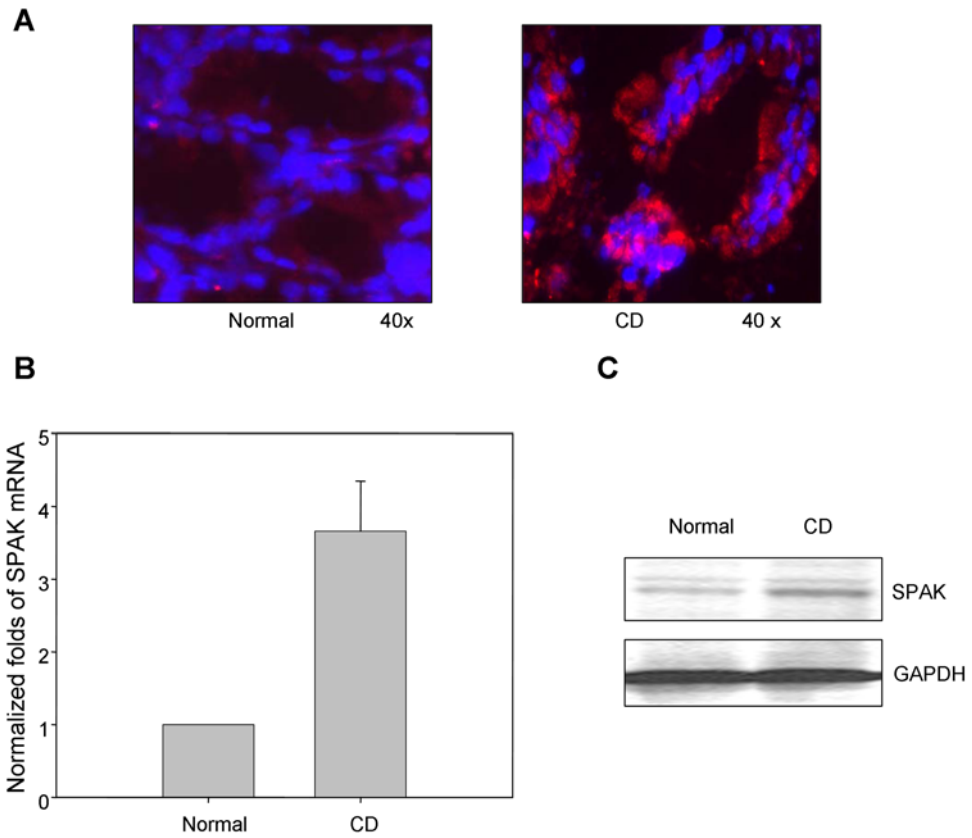

Figure 1. SPAK expression profile in colon tissue from patients with ulcerative colitis. A. Immunostaining of SPAK in normal human colon tissue and Crohn's disease (CD) patient colon tissue from mucosal biopsies. SPAK expression (red); nuclear staining by DAPI (blue); SPAK is primarily expressed in epithelial cells. **B.** The expression of SPAK mRNA in normal human and Crohn's disease (CD) patient colon tissues from mucosal biopsies were quantified by real-time PCR, ** $p<0.01$. **C.** 30 μg of protein from normal human colon and Crohn's disease (CD) patient colon from mucosal biopsies were examined by western blot with SPAK antibody, colon tissue from CD patients demonstrated significantly higher levels of SPAK expression (upper part) vs. healthy colon, with GAPDH as the internal loading control.
doi:10.1371/journal.pone.0005049.g001

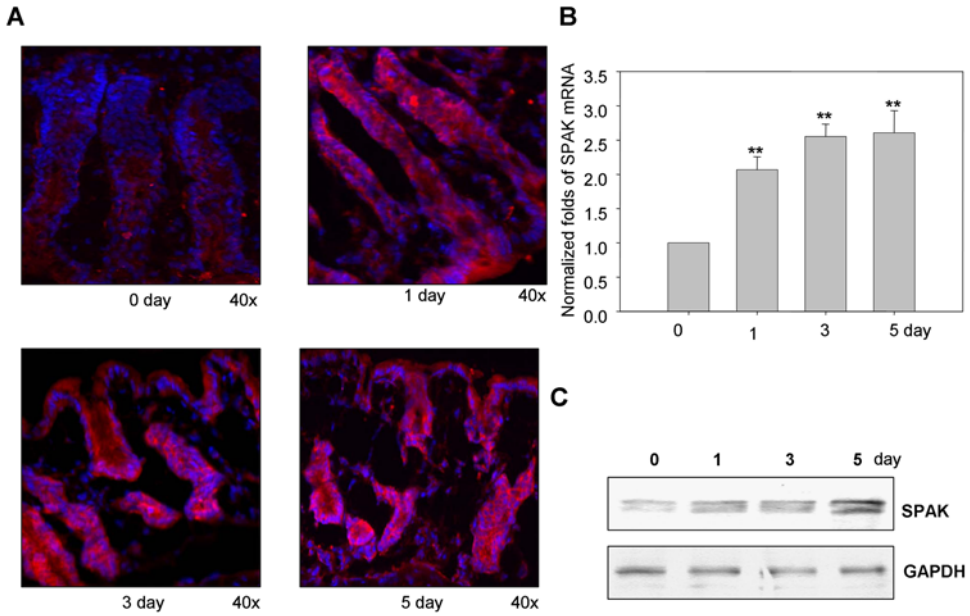

Figure 2. SPAK expression profile in colon tissue from mice treated with hyperosmolarity. A. Immunostaining of SPAK in colon sections of mice treated with hyperosmolarity at 0, 1, 3, and 5 days. SPAK (red); nuclear staining by DAPI (blue). **B.** Real time PCR analysis of SPAK mRNA expression in mucosa from colon tissue of hyperosmolarity treated mice. ** $p<0.01$. **C.** Western blot analysis of SPAK (upper part) expression in mucosa from colon tissue of hyperosmolarity treated mice, with GAPDH as the internal loading control.
doi:10.1371/journal.pone.0005049.g002

Hyperosmolarity increases SPAK expression in intestinal epithelial cell lines *in vitro*

Actin plays an important role in cell shape, volume and regulation of barrier function through interaction with tight-junction proteins; hence we examined the effects of hyperosmolarity on distribution of actin and expression levels of SPAK. We found that hyperosmolarity treatment leads to increased levels of Triton x-100-insolube F-actin and an increased ratio of F-actin versus G-actin (Fig. 3A). The newly polymerized F-actin predominantly localizes to the plasma membrane, where it forms a thick ring [38,39] that persists as long as hyperosmolarity is maintained. Furthermore, immunofluorescence showed that hyperosmotic treatment leads to Caco2-BBE cell shrinkage and increases the intercellular space. Importantly, hyperosmotic conditions significantly increased SPAK expression levels and recruitment of SPAK to the membranes of cells (Fig. 3A). SPAK mRNA and protein levels were also increased, reaching maximum level as early as 3 min after hyperosmotic treatment (Fig. 3B, 3C and 3D). Here, we cannot conclude whether the high SPAK level was due to new synthesis or recruitment of SPAK to the membrane, or both. Under hyperosmotic conditions, SPAK levels increase in Triton x-100-soluble and insoluble pool, indicating SPAK recruitment to the F-actin-associated pool (Fig. 3E). Together, these data show that, under hyperosmotic conditions, increased SPAK is redistributed to actin-containing regions of the plasma membrane.

Induction of SPAK is primarily at the transcriptional level

To determine whether the induction of SPAK expression under hyperosmotic conditions was mediated by transcriptional or post-transcriptional mechanisms, nuclear run-on assays (Fig. 4A) were performed in Caco2-BBE cells pretreated with or without hyperosmotic conditions. Compared with nuclei not exposed to hyperosmotic conditions, exposure to hyperosmotic conditions increased SPAK mRNA levels. This experiment was repeated three times and similar results were obtained each time. These results indicate that this increase in SPAK levels is due to increased transcription.

The increase of SPAK transcription by hyperosmolarity is not mediated by alteration of mRNA stability

Changes in steady-state mRNA levels may be due to changes in the degradation rate of a transcript and/or rate of gene transcription. Hence, it was important to investigate the relative contribution of post-transcriptional mechanisms in the modulation of SPAK mRNA levels by hyperosmolarity. To assess SPAK mRNA stability, Caco2-BBE cells were treated with 5 μg/ml of AcD to inhibit mRNA synthesis, and SPAK mRNA levels were measured at the indicated time points in the presence and absence of hyperosmolarity by real-time RT-PCR; 18S rRNA was used as an internal control to normalize SPAK mRNA levels. The decay rate of SPAK mRNA in AcD-treated Caco2-BBE cells was almost the same as that of SPAK mRNA in cells treated with AcD plus hyperosmolarity; no significant difference was detected (Fig. 4B). In parallel, Northern-blot analyses were performed on 20-μg samples of Caco2-BBE mRNA treated with or without AcD (5 μg/ml) and/or exposed to hyperosmotic conditions (Fig. 4C). Results showed that AcD can significantly reduce mRNA levels (Fig. 4C lane 2) compared with untreated Caco2-BBE cells (Fig. 4C lane 1). In addition, hyperosmolarity treatment (in the absence of AcD treatment) markedly increased levels of SPAK mRNA transcripts. However, if Caco2-BBE cells were pretreated with AcD for 1 hour, hyperosmolarity cannot reverse the AcD-induced mRNA degradation. Together, these findings indicate that the observed changes in SPAK protein level are due to increased SPAK mRNA transcription rather than changes in mRNA stability.

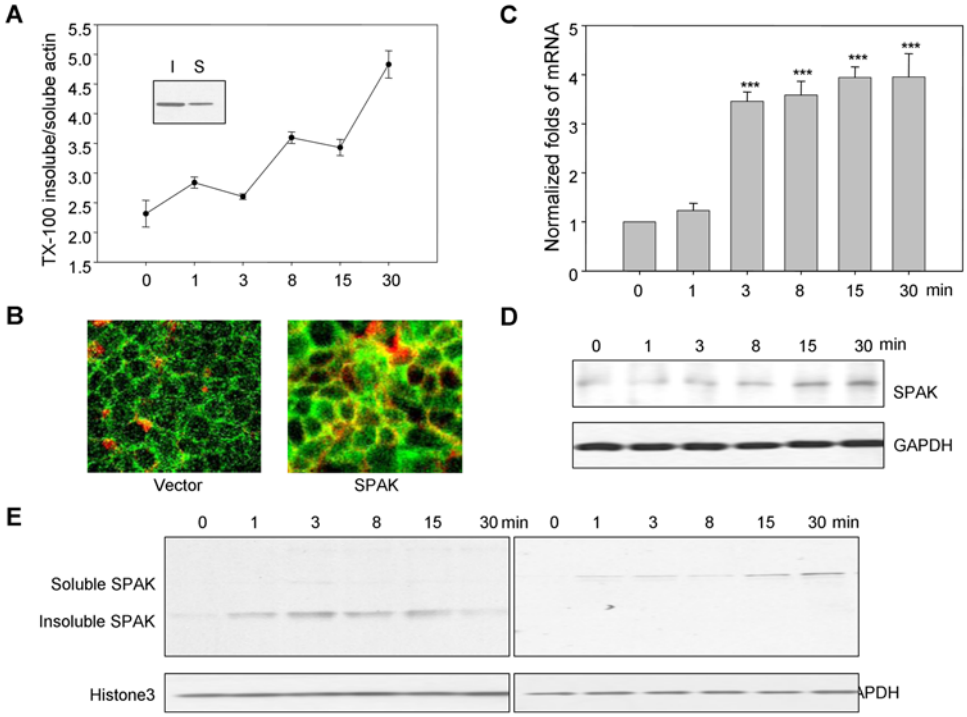

Figure 3. SPAK expression in hyperosmolarity treated Caco2-BBE cells. A. Graph of ratio of triton x-100 insoluble actin *v.s.* soluble actin and western blot. **B.** Immunostaining of SPAK in colonic Caco2-BBE cells treated with hyperosmolarity at 0 and 15 min. SPAK (green); actin by rhodamine (red). (C) Real time PCR and (D) Western blot demonstrated that treatment of hyperosmolarity increases SPAK expression with GAPDH as internal loading control, ** $p<0.01$, *** $p<0.001$. E. Western blot showed that SPAK expression is increased by hyperosmolarity and is recruited to the triton-100 insoluble pool at 0, 1, 3, 8, 15 and 30 min.
doi:10.1371/journal.pone.0005049.g003

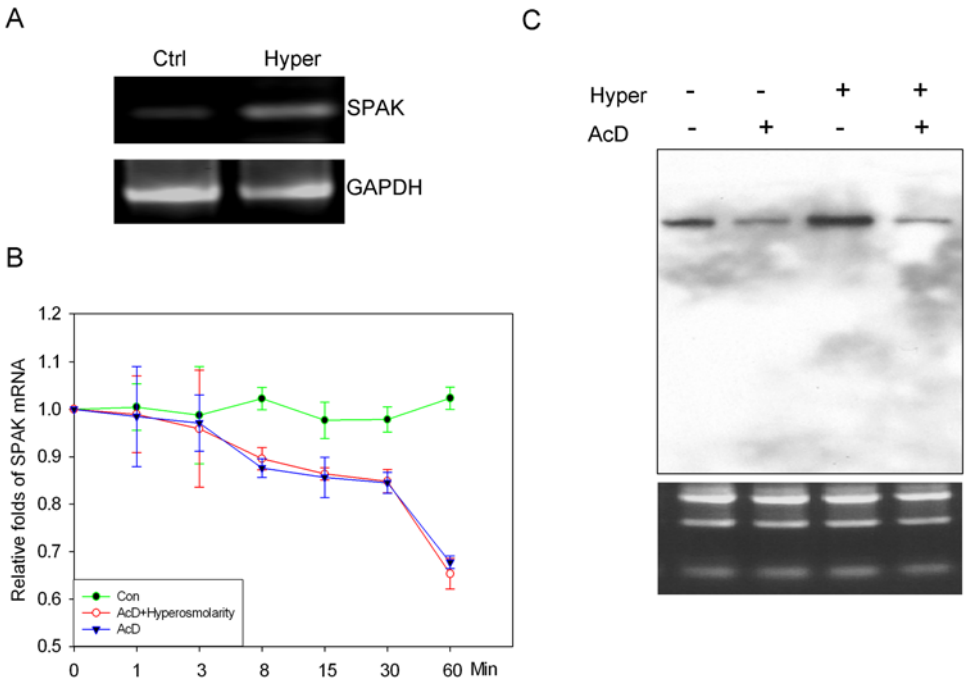

Figure 4. Hyperosmolarity regulates SPAK expression at the transcriptional level. A. Nuclear run-on assay indicated the increase of SPAK mRNA transcription under the treatment of hyperosmolarity, with the mRNA transcription of GAPDH as internal control. **B.** Hyperosmolarity does not change SPAK mRNA stability; the percentage of remaining SPAK mRNA is shown at the different time point. Solid circle represents the value of real time PCR with the samples from Caco2-BBE cells without treatment, open circle represents the value of real time PCR with the samples from Caco2-BBE treated with actinomycin D, solid triangle represents real time PCR with the samples from Caco2-BBE treated with actinomycin D and hyperosmolarity. **C.** Northern blot analysis of total RNA from Caco2-BBE cells, Lane 1, no treatment, Lane 2, AcD, Lane 3, hyperosmolarity, and Lane 4, AcD and hyperosmolarity. The lower RNA electrophesis shows equal loading of each condition.
doi:10.1371/journal.pone.0005049.g004

Sp1- and NF-κB-binding sites have roles in SPAK promoter activity

Having demonstrated that hyperosmolarity-induced SPAK expression is regulated at the transcriptional level, we cloned a ~1.5-kb fragment of the 5′-flanking region of the SPAK gene from human genomic DNA to further understand the molecular mechanisms underlying the increased expression of SPAK. To identify the core promoter region of the SPAK gene, we generated five partial deletion constructs fused with the luciferase reporter gene. Caco2-BBE cells were transiently transfected with these constructs, then stimulated by exposure to hyperosmotic conditions (610 mOsm) for 30 min. Transcriptional activities were then measured using the Dual-Luciferase Reporter Assay System (Promega, San Luis, CA). The full-length promoter displayed increases of ~18-fold in basal promoter activity and 74-fold in hyperosmolarity-stimulated promoter activities, compared with the empty pGL3 basic vector (Fig. 5A and 5B). Constructs I, II, III, IV and V had ~16, 9, 10, 6 and 1-fold greater promoter activities, respectively, compared with the pGL3 vector at the basal level. Under hyperosmotic conditions, constructs I and II showed ~70 and 53-fold increases, respectively, in promoter activity compared with the basic vector pGL3, to give activities that were about 95% and 72%, respectively, of the activity of the full-length SPAK promoter. The basal and hyperosmolarity-induced promoter activities of constructs III, IV and V were greater than those of the pGL3 vector (~26, 20, 4-fold increases, respectively); however, the activities were only about 35%, 27% and 6%, respectively, of that of the full-length SPAK promoter (Fig. 5B). To investigate and confirm the functional roles of the relevant binding motifs in regulating SPAK promoter activity, we generated various Sp1- and NF-κB-binding mutants (Fig. 5C). Using the transcriptional activity assay, we found that all the Sp1 mutants had significantly reduced basal promoter activities compared with the wild-type promoter, and the hyperosmolarity-stimulated activity levels of these Sp1 mutants were also lower than the wild-type promoter activity (Fig. 5C and 5D). By contrast, although the NF-κB mutant basal luciferase activity was similar to that of the wild-type promoter, there was a marked reduction in

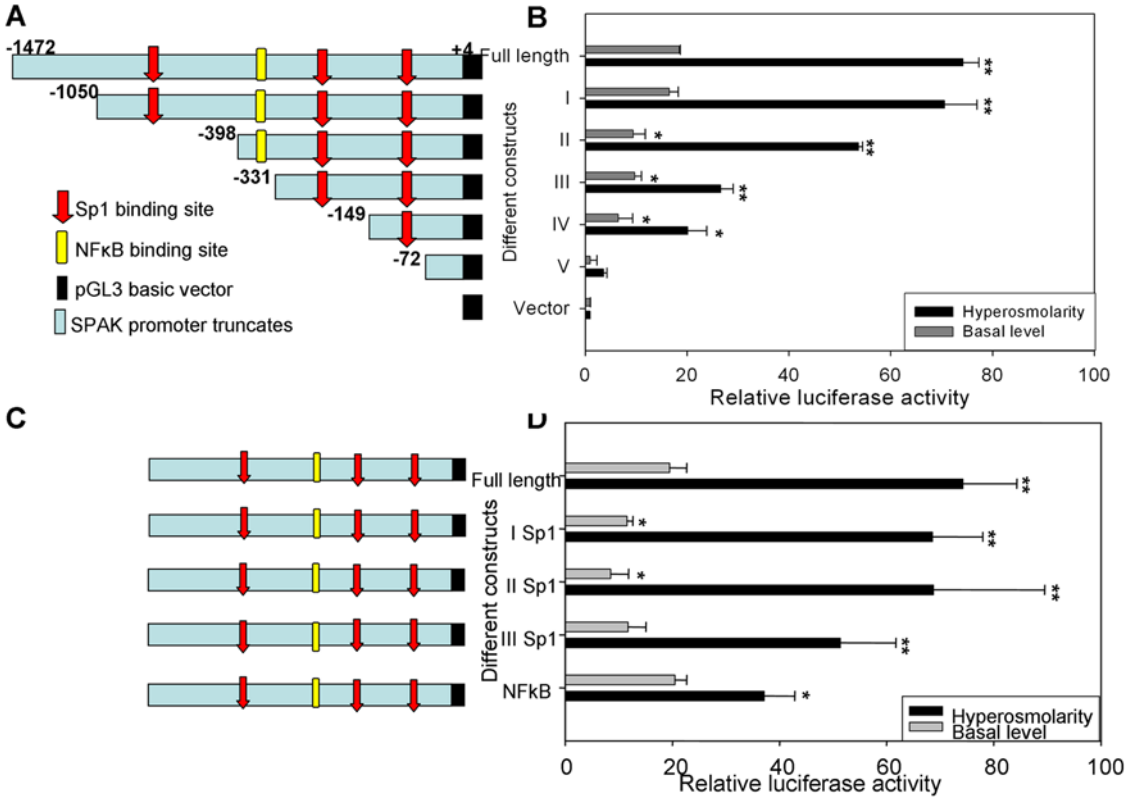

Figure 5. Characterization of SPAK promoter. A. Schematic representation of human SPAK promoter constructs. the full-length SPAK promoter (nt-1472 to +4); construct I (nt −1050 to +4); construct II (nt −398 to +4); construct III (nt −331 to +4); construct IV (nt −149 to +4) and construct V (nt −72 to +4). Numbers are given in relation to the translational start codon (+1) and indicate 5′-ends of the deletion constructs. The location of the identified positive regulatory region is indicated by a light blue box. Positions of the putative Sp1 (Red) and NF-κB (Yellow) sites are indicated by arrows. **B.** Promoter activities of the 5′ deleted constructs in un-treated or hyperosmolarity-stimulated Caco2-BBE cells normalized to *Renilla* Luc activities driven by the phRL-CMV control vector. Activities are expressed as fold inductions over cells transfected with the empty pGL3-basic vector. Each value represents the mean±SD of at least 3 independent sets of transfection experiments performed in triplicate, *$p<0.05$; **$p<0.01$. **C.** Schematic representation of mutated SPAK promoter constructs: the full-length SPAK promoter; I Sp1 binding site (−496); II Sp1 binding site (−303); III Sp1 binding site (−114) and NF-κB binding site (−354). The digits are given in relation to the translational start codon (+1). The location of the identified positive regulatory region is indicated by a light blue box. Positions of the putative Sp1 sites are indicated by arrows and NF-κB is indicated by rectangle. The corresponding mutated transcription factor binding site is indicated by black arrow or black rectangle. **D.** Effects of mutations of Sp1 or NF-κB binding sites on SPAK promoter activity. The various mutated constructs were transiently transfected into Caco2-BBE cells under the basal (gray bar) or hyperosmolarity conditions. Promoter activity of the full-length wild-type construct was set to 100% (control). Values represent means±SD of at least 3 independent sets of transfection experiments performed in triplicate, *$p<0.05$, **$p<0.01$.
doi:10.1371/journal.pone.0005049.g005

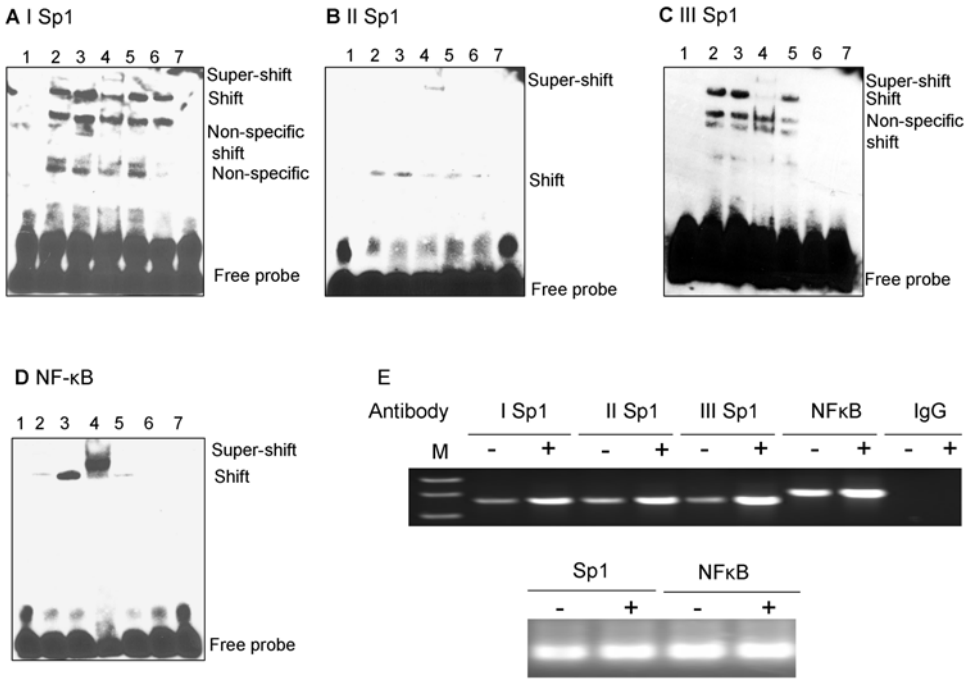

Figure 6. EMSA of (A) I Sp1 (−496), (B) II Sp1 (−303), (C) III Sp1 (−114), (D) NF-κB (−354). Lane 1, biotin-labeled oligonucleotide alone; lane 2, biotin-labeled oligonucleotides incubated with 5 μg Caco2-BBE nuclear extracts; lane 3, biotin-labeled oligonucleotides incubated with 5 μg hyperosmolarity-treated Caco2-BBE nuclear extracts; lane 4, biotin-labeled oligonucleotides incubated with 5 μg Caco2-BBE nuclear extracts in the presence of anti-Sp1 (**A–C**) or NF-kB (p65) (**D**) antibodies; lane 5, biotin-labeled oligonucleotides incubated with 5 μg Caco2-BBE nuclear extracts in the presence of non-specific IgG; lane 6, biotin-labeled oligonucleotides incubated with 5 μg Caco2-BBE nuclear extracts in the presence of a 50-fold excess of cold competitor oligonucleotide; lane 7, biotin-labeled binding site-mutated oligonucleotides incubated with 5 μg Caco2-BBE nuclear extracts. **E.** Chromatin immunoprecipitation (ChIP) assay: the antibodies indicated were incubated with cross-linked DNA isolated from Caco2-BBE cells treated with (+) or without (−) hyperosmolarity, IgG antisera acts as control. Sp1 (I, II, and III) and NF-κB promoter elements in the immunoprecipitates were detected by PCR. The lower panel shows DNA input as template for internal control.
doi:10.1371/journal.pone.0005049.g006

hyperosmolarity-stimulated promoter activity (~50% reduction) (Fig. 5D). Taken together, these results show that the Sp1-binding sites are important in basal and stimulated SPAK promoter activities, and that the NF-κB-binding site has a crucial role in hyperosmolarity-stimulation of SPAK promoter activities.

Sp1 and NF-κB are physically associated with their corresponding binding sites

To study the association between the transcription factors and the corresponding binding sequences, and to further confirm the importance of Sp1 and NF-κB in activation of the SPAK gene, we used electrophoretic mobility shift assays (EMSA) to characterize binding of Sp1 and NF-κB to their respective binding sites: Sp1 −496 (Fig. 6A), Sp1 −303 (Fig. 6B), Sp1 −114 (Fig. 6C), and NF-κB −354 (Fig. 6D). EMSA revealed that incubation of the DNA–protein complexes with anti-Sp1 or anti-p65 antibodies shifted the migrating bands in an upward direction, indicating specificity for Sp1 and NF-κB (p65) proteins (Fig. 6A, 6B, 6C and 6D, lane 4). Exposure to hyperosmotic conditions for 30 min increased the binding of Sp1 to the corresponding oligonucleotides compared with the untreated control (Fig. 6A, 6B and 6C, lane 3). This indicates that hyperosmolarity increases Sp1 expression or binding of Sp1 to oligonucleotides. Similarly, as shown in Fig. 6C, hyperosmolarity treatment increases NF-κB (p65) binding to the corresponding oligonucleotides. To confirm the *in vivo* importance of Sp1 and NF-κB (p65) binding sites in response to hyperosmolarity, we performed chromatin immunoprecipitation (ChIP) analyses. As shown in Fig. 6E, under resting conditions, Sp1 binds to the I Sp1 (lane 1), II Sp1 (lane 3), and III Sp1 (lane 5) binding sites and NF-κB (p65) binds to the NF-κB-binding site (lane 7). Hyperosmolarity treatment increases the DNA-binding activities of Sp1 and NF-κB (p65) to their binding sites. Together, these results indicate that Sp1 and NF-κB binding increases under hyperosmotic conditions. These data, together with the results of the promoter studies, demonstrate the critical role of Sp1 and NF-κB in the regulation of basal and hyperosmolarity-induced SPAK expression.

Hyperosmolarity increases SPAK expression via increased NF-κB expression *in vivo*

To confirm the effects of hyperosmolarity on SPAK expression, nuclear proteins were extracted from colonic epithelial cells of mice treated exposed to hyperosmotic conditions and subjected to Western-blot analysis with Sp1 and NF-κB antibodies. As shown in Fig. 7A, after different durations of hyperosmolarity exposure, there was no significant change in the Sp1 protein level; however, expression of NF-κB (p65) increased as early as the first day. These *in vivo* data show that hyperosmolarity does not affect the overall nuclear levels of Sp1; however, hyperosmolarity treatment induces translocation of NF-κB (p65) to the nucleus and upregulates its expression level. These results were confirmed with Caco2-BBE cells exposed to hyperosmotic conditions. As shown in Fig. 7B, hyperosmotic medium significantly increases NF-κB (p65) expression levels, but not Sp1 levels. Together, the *in vivo* and *in vitro* studies demonstrate that hyperosmolarity regulates SPAK in a NF-κB-dependent manner.

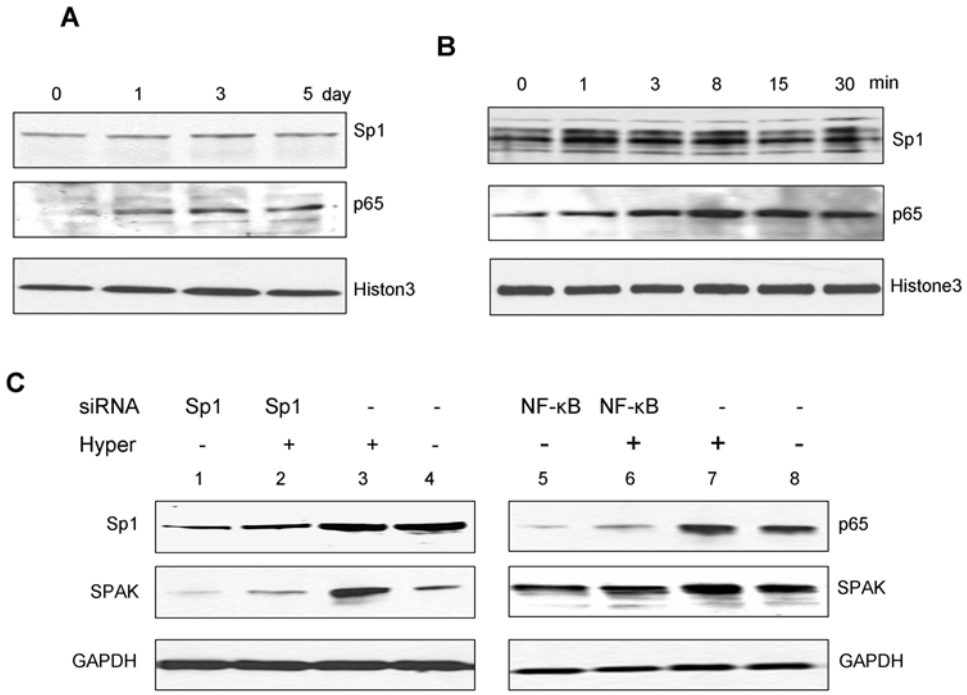

Figure 7. Western blots of transcription factors Sp1 and NF-κB (p65). A. Western blots of Sp1 and NF-κB (p65) demonstrating hyperosmolarity effect on Sp1 and NF-κB protein levels *in vivo*. Histone3 acts as a control. **B.** Western blots of Sp1 and NF-κB (p65) demonstrating hyperosmolarity effect on Sp1 and NF-κB protein levels *in vitro*. Histone3 acts as a control. **C.** Reduction of NF-κB but not Sp1 expression reduced SPAK protein expression in unstimulated and in hyperosmolarity-stimulated Caco2-BBE cells. Cells were harvested and subjected to western blot analysis using Sp1, NF-κB (p65), and SPAK antibodies as described in materials and methods. GAPDH acts as a loading control.
doi:10.1371/journal.pone.0005049.g007

Reduction of Sp1 or NF-κB expression differentially regulates SPAK expression

One approach to studying the functional role of a specific protein is to knockdown its expression. To further study SPAK regulation by Sp1 and NF-κB, we used siRNA to prevent Sp1 and NF-κB expression. As shown in Fig. 7C, Caco2-BBE cells transfected with siRNA against Sp1 and NF-κB (p65) showed decreased expression levels of Sp1 (lanes 1 and 2) and NF-κB (p65) (lanes 5 and 6) compared with Caco2-BBE cells transfected with scrambled control siRNA. Basal SPAK protein expression was also significantly reduced in Caco2-BBE cells transfected with Sp1-specific siRNA (SPAK lane 1 vs lane 4); however, there were no significant reductions in SPAK expression in cells transfected with NF-κB (p65)-specific siRNA (SPAK lane 5 vs lane 8). Thus, basal SPAK expression is effectively reduced by reduced levels of Sp1. We further investigated whether siRNA against Sp1 and/or against NF-κB reduced the levels of hyperosmolarity-induced SPAK expression. As shown in Fig. 7C, hyperosmolarity-induced SPAK expression levels were significantly reduced in Caco2-BBE cells transfected with Sp1-specific siRNA or NF-κB-specific siRNA (SPAK lanes 2 and 6, respectively) compared with cells transfected with scrambled siRNA (SPAK lane 3 and 7). These data demonstrate that Sp1 has an important role in the basal expression of SPAK, and Sp1 and NF-κB have important roles in the transcriptional regulation of SPAK expression under hyperosmotic conditions.

SPAK expression regulates epithelial barrier function *in vitro*

On the basis of our data showing that SPAK expression is increased in colonic tissue of CD patients, we hypothesized that SPAK may play a role in epithelial barrier function. We studied permeability in Caco2-BBE cells stably transfected with SPAK/pcDNA6, vector pcDNA6, SPAK siRNA or Con siRNA using a fluorescein isothiocyanate (FITC)-labeled dextran method (Fig. 8A

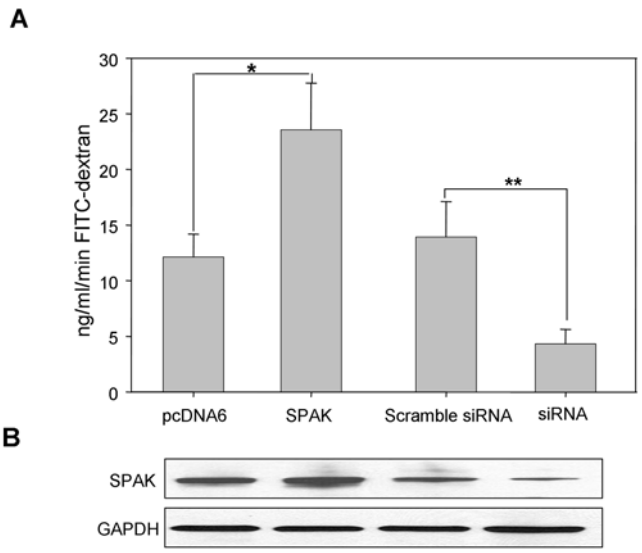

Figure 8. SPAK is involved in epithelial barrier function *in vitro*. A. *In vitro* permeability assay in Caco2-BBE cells transfected with pcDNA6, SPAK/pcDNA6, con siRNA or SPAK siRNA with 4 kDa FITC-Dextran. Fluorescence was quantified in lower chamber at 2 hours after the administration of FITC-dextran (λ ex = 492 nm, λ em = 510), *$p<0.05$, **$p<0.01$. **B.** Western blot of Caco2-BBE cells protein scraped from filter after the *in vitro* permeability assay.
doi:10.1371/journal.pone.0005049.g008

and 8B), as described in the *Materials and Methods*. Fluorescence was quantified in the lower chamber 2 hours after the administration of FITC–dextran. As shown in Fig. 8A, vector-transfected cells showed an FITC-dextran level of 12.1±2.6 ng of FITC/ml protein/min. In comparison, there was a ~2-fold increase in FITC-dextran levels in SPAK/pcDNA6-transfected cells (23.8±4.03 ng of FITC/ml protein/min), almost no change in FITC–dextran levels in Con-siRNA-transfected cells (13.9±3.2 ng of FITC/ml protein/min), and a ~3.2-fold decrease in FITC–dextran levels in SPAK-siRNA-transfected cells (4.3±1.3 ng of FITC/ml protein/min). These results indicate that overexpression of SPAK increases the permeability of cells and reduced SPAK expression decreases the permeability.

SPAK expression regulates epithelial barrier function *in vivo*

Transgenic mice have been widely used as a robust, dependable animal model of human disease. To better understand the function of SPAK in IECs, we generated transgenic mice that expressed a constitutively active form of SPAK under the control of the *villin* gene locus control region (LCR), which can target SPAK expression only in IECs (as shown in Fig. 9A, 9B and 9C) at the mRNA and protein levels, as described previously [40]. Our data demonstrated that Caco2-BBE cells stably transfected with SPAK showed increased permeability *in vitro*, so it was important to study the role of SPAK in epithelial barrier function in mice. With SPAK transgenic FVB/6 mice harboring the *villin* gene, which limits SPAK overexpression in the intestine, we studied barrier function in wild-type and SPAK transgenic mice using the FITC-labeled dextran method, as described in the *Materials and Methods*. Mice were administered FITC–dextran by gavage, and fluorescence was quantified in the serum 4 h after administration. As shown in Fig. 9D, wild-type mice had a FITC–dextran level of 0.805±78 mg /μg protein. By contrast, SPAK transgenic mice showed a ~4.5-fold increase in the FITC–dextran level (3.469±234 mg /μg protein), indicating decreased barrier function in these mice.

Discussion

In this study, we demonstrated for the first time that colonic SPAK expression levels are increased in mucosal biopsy samples of patients with CD. It is known that patients with CD have markedly higher colonic osmolarity compared with healthy individuals [1,2,3], and this high colonic osmolarity contributes to the activation of colonic mucosal inflammation in Crohn's colitis [1,4]. This high osmolarity also led to increased expression of colonic SPAK in mice and a Caco2-BBE cell model, and the SPAK expression level was correlated with the extent of colonic mucosa injury. We can conclude that hyperosmolarity can upregulate the SPAK expression. Hyperosmolarity can also regulate the expression of other molecules; examples of such regulation include upregulation of yeast alpha-glycerophosphate dehydrogenase 1 (GPD1) [41], upregulation of IL-8 in bronchial epithelial cells [8], peripheral blood mononuclear cells [7] and the intestinal epithelial cell lines Caco2-BBE and HT29 [10], upregulation of the taurine transporter (TauT) in ARPE-19 cells [42], upregulation of MMP-9 in human corneal epithelial cells [6], and downregulation of the cystic fibrosis transmembrane conductance regulator (CFTR) in HT29 and T84 cells [43].

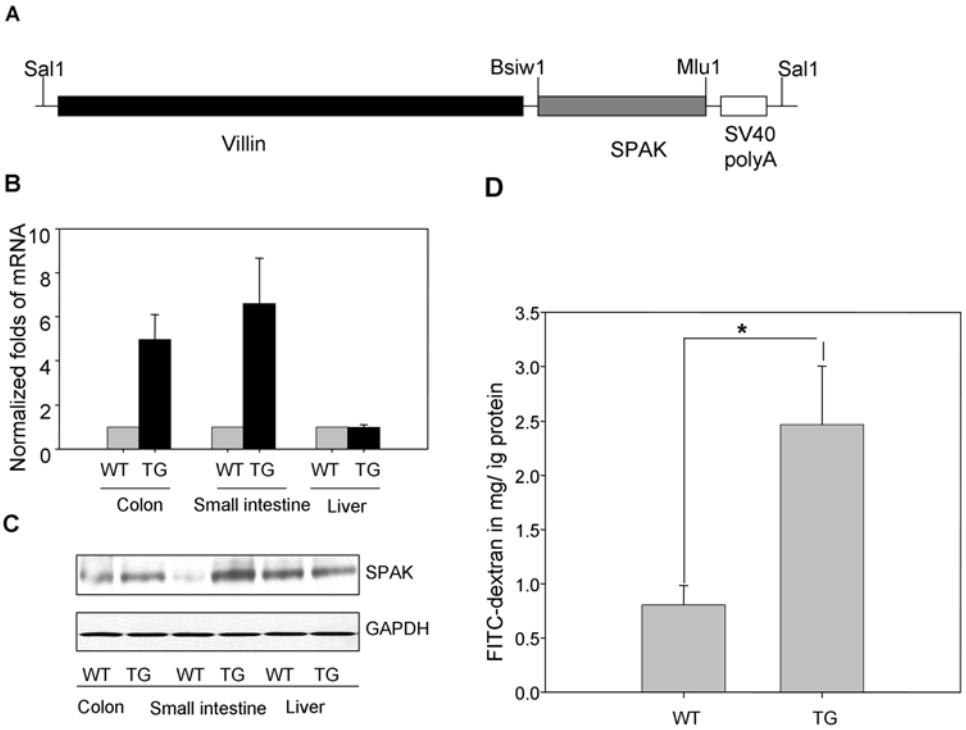

Figure 9. SPAK is involved in epithelial barrier function *in vivo*. **A.** Schematic diagram of villin/SPAK transgene construct, full length SPAK cDNA was cloned into villin vector by *Bsiw1/Mlu1* sites; villin/SPAK was digested with *Sal1* before microinjection. **B.** SPAK is tissue-specifically over-expressed in intestine by real time PCR with samples from small intestine, colon and liver. **C.** SPAK is specifically over-expressed in intestine by western blot with samples from small intestine, colon and liver. **D.** *in vivo* permeability assay in villin/SPAK transgenic mice, WT: wide type; TG: transgenic mice, ** $p<0.01$.
doi:10.1371/journal.pone.0005049.g009

We used the SPAK TATA-less promoter to study the mechanisms underlying the hyperosmolarity-induced changes in SPAK expression during intestinal inflammation. We found that Sp1 binding sites are important both for basal and hyperosmolarity-induced promoter activities, whereas the NF-κB binding site plays an important role in the hyperosmolarity-induced promoter activity. Sp1 is known to support constitutive expression of a variety of eukaryotic genes that lack a functional TATA box and is thought to have key roles in regulating the expression of both house-keeping [44,45] and non-house keeping genes [46]. NF-kB comprises a family of proteins that form a variety of hetero- and homodimers, the subunits of which upregulate gene transcription induced by inflammatory stimuli such as cytokines, bacterial products, viral expression, growth factors, and other stress stimuli in an NF-κB-dependent manner [47,48]. Transcription of several genes is upregulated, including those encoding the proinflammatory cytokines IL-1, IL-6, IL-12, TNF-α, IFN-γ and IL-8, the chemokine MIP-1 and the adhesion molecule ICAM [49,50,51]. NFκB has also been shown to be involved in the regulation of inflammatory responses in IBD [52,53]. NFκB is known to function together with cooperating transcription factors and coactivators, such as Sp1, to activate transcription [54,55,56]. For example, NF-κB can interact with Sp1 [57] to regulate HIV-1 [46], ICAM1 [58,59], and granulocyte macrophage colony-stimulating factor 1 (GM-CSF); the interaction involves the zinc finger region of Sp1 and the N-terminal Rel homology domain of p65 [54]. Under certain conditions, NF-κB can also bind to the consensus sequence of the Sp1 binding site, thereby competing with Sp1 [60,61].

We found that hyperosmolarity does not affect the overall nuclear levels of Sp1 in mice or Caco2-BBE cells, in agreement with previous results [62]. However, under hyperosmotic conditions the expression and translocation of NF-κB into the nucleus were increased [10,15,63], which indicates that increased expression of SPAK is, at least in part, due to increased expression of NF-κB as well as increased binding of Sp1 and NF-κB to their binding sites. Our data also show that knock-down of NF-κB (p65) or Sp1 by siRNA can significantly decrease SPAK expression levels, confirming their importance in the regulation of SPAK expression and indicating their potential as a target for the treatment of inflammatory diseases such as IBD [52,64,65,66,67]. Our results additionally demonstrate that NF-κB and Sp1 transcription factors are essential for regulation of SPAK expression under hyperosmotic conditions. However, SPAK expression may be regulated by multiple transcription factor pathways because we have previously reported that TNF-α-regulated SPAK expression is NF-κB-dependent but Sp1-independent [29].

Nuclear run-on assays are commonly used to determine whether an increase in mRNA level is due to an increase in transcription, a decrease in the degradation rate, or both. For example, mRNA levels in *Drosophila* [68] were found to be regulated at a post-transcriptional level without evident transcriptional regulation; however, simultaneous inhibition of both Erk and p38 kinase pathways decreased the levels of cytokine gene transcription (IL-6 and TNF-α) [69]. Our data show that exposure to hyperosmotic conditions (for 60 min) significantly increases SPAK mRNA transcription, which is in agreement with previous reports that osmolarity does not affect mRNA stability or enzyme degradation [70,71]. However, hyperosmolarity can regulate the expression of target genes by several different mechanisms; for example, the transcriptional decrease in mRNA levels of CFTR [43] and TauT [42], and induction of IL-8 through activation of NF-κB in a p38-kinase-dependent manner [8,10].

Hyperosmolarity has multiple and complex cellular effects. For example, hyperosmolarity decreases Na^+ transport and impairs barrier function of sheep rumen epithelium [72]; however, it increases the lung capillary barrier [73]. The mechanisms underlying the various aspects of barrier function affected by hyperosmolarity are complicated. First, hyperosmolarity activates the p38 and JNK pathway (Figure S1), as demonstrated previously [8,10,13,43,74,75], which in turn can lead to increased epithelial permeability. Second, hyperosmolarity induces the production of proinflammatory cytokines such as TNF-α, IL-1β, IL-6, IL-8 (Figure S2) that disrupt epithelial barrier function, as described previously [10,12,13,16,76]. Third, hyperosmolarity can induce apoptosis, resulting in the loss of barrier function [16,75,77]. However, in agreement with previous reports, in the present study hyperosmolarity also activated the Erk1/2 pathway (Figure S1) [75,78,79,80], which is involved in the mechanism by which permeability is decreased [81]. Furthermore, hyperosmolarity leads to redistribution and polymerization of cortical F-actin, which is involved in the downregulation of cellular permeability [82,83,84]. Hyperosmolarity can induce activation of focal adhesion kinase and redistribution of focal adhesion protein, which can lead to increased barrier function [85,86]. Finally, in the present study, hyperosmolarity (610 mOsm, 30 min) did not induce significant apoptosis in Caco2-BBE cells (Figure S3), which eliminates the possibility that this pathway increases epithelial permeability.

Here we showed that upregulation of SPAK expression is directly involved in the regulation of intestinal barrier permeability. As demonstrated using the FITC–dextran method in Caco2-BBE cells and transgenic mice, SPAK can cause severe barrier dysfunction. Transgenic mice harboring the SPAK gene under control of the *villin* gene utilize the tissue-specific expression of villin in the intestinal epithelium, which facilitates transgenic SPAK expression in a tissue-specific manner [40] without causing unexpected results in other tissues. The barrier dysfunction caused by SPAK overexpression is important because it has a central role in the pathogenesis of intestinal inflammation [87,88,89]. Different mechanisms may underlie the SPAK-induced increase in transepithelial permeability, including activation of the p38 pathway [27,28], which can increase epithelial permeability. A strong link has been established between the p38 pathway, cell volume change and inflammation [8,10,90,91], as well as in the regulation of cell motility and wound healing [45,92,93].

In conclusion, we report that during inflammatory diseases (such as IBD) and hyperosmotic conditions, the SPAK expression level was significantly upregulated at the transcriptional level due to multiple factors, including the transcription factors NF-κB and Sp1. Our data demonstrate that SPAK expression is upregulated by hyperosmolarity and is an important mediator of barrier function. SPAK expression may thus contribute to the pathogenesis of intestinal inflammatory diseases such as IBD.

Materials and Methods

Human material

The diagnosis of IBD was based on clinical, endoscopic, and histological criteria. Clinical data for IBD patients were obtained by medical record review. Infectious colitis was ruled out by stool cultures. The collection of samples was approved by the Institutional Review Board of Emory University. Mucosal biopsy specimens from 4 Crohn's disease active patients were obtained during routine endoscopy that was performed after written informed consent was obtained. Control biopsy samples were collected from 6 volunteers undergoing colonoscopy for colorectal

cancer screening who had no overt pathology including polyps. Biopsy specimens were snap frozen in Optimal Cutting Temperature immediately after endoscopic resection and stored at −80°C for histological immunostaining or homogenized to extract protein for western immunoblotting or RNA for real time PCR.

Mouse model

C57BL/6 and FVB/6 mice (8 wk, 18–22 g) obtained from Jackson Laboratories (Bar Harbor, ME). Mice were group housed under a controlled temperature (25°C) and photoperiod (12:12-h light-dark cycle) and allowed unrestricted access to standard mouse chow and tap water. They were allowed to acclimate to these conditions for at least 7 days before inclusion in the experiments. All animal experiments were approved by The Institutional Animal Care and Use Committee of Emory University, Atlanta and were in accordance with the guide for the Care and Use of Laboratory Animal, published by the U.S. Public Health Service. Groups of mice ($n = 6$ mice/group) were treated with hyperosmotic medium (610 mOsm) prepared by dissolving mannitol (0.3 M) in phosphate buffered saline (PBS) for indicated days.

Generation of transgenic mice

The full-length human colonic SPAK cDNA [28] spanning from nucleotide 139 to 1569 was introduced into the *BsiWI/MluI* site of pBS KS Villin MES SV40 polyA vector [40] harboring the *villin* gene, the villin promoter can target SPAK over expression in *villin*-containing intestine. The transgene SPAK digested with *SalI* were injected into the pronuclei of the fertilized eggs of the FVB/6 mice in collaboration with the Transgenic Mouse and Gene Targeting Core Facility (Emory University). Transgene-carrying mice were identified by PCR of genomic DNA extracted from mice tails with REDExtract-N-Amp Tissue PCR kit (Sigma-Aldrich, ST. Louis, MO). The primers were: Prim1F (5′ GGCTGTGATAGCACACAGGA 3′) and Prim1R (5′ CTGCCTGAACCACAGCAGTA 3′) or Prim2F (5′ TGGGTTTGCTCAGTTGAGTG 3′) and Prim2R (5′ AGTCGACGAATTCCGATTTG 3′). Stable SPAK-transgenic lines were established by backcrossing transgene-carrying founder mice with FVB/6 mice (Jackson Laboratories, Bar Harbor, ME).

Cell culture

Human intestinal cell line Caco2-BBE was cultured according to the standard protocol. Caco2-BBE cells were treated with isosmolar medium or hyperosmotic mdium (610 mOsm) prepared by adding 0.3 M mannitol (Sigma-Aldrich, ST. Louis, MO) to regular Dulbecco's modified Eagle's medium DMEM (Invitrogen, Carlsbad, CA).

Plasmids construction

SPAK promoter, its different truncates and site-directed mutants were cloned and constructed in our lab previously [29].

Western blot

Western blot were carried out based on the standard methods with relevant antibodies.

Immunohistochemistry

Immunostaining was performed according to the standard protocol. Briefly, 7-μm cryostat sections of mouse colon were fixed in buffered 4% paraformaldehyde for 30 min, blocked specimen in 5% normal rabbit serum in PBS/Triton for 1 h, and incubated with rabbit SPAK antibody (Cell signalling technology Inc, Danvers, MA) overnight at 4°C, washed with phosphate-buffered saline (PBS), and subsequently incubated with fluoresceinated secondary antibody for 1 h at room temperature. Colon sections were stained with 4′, 6-Diamidine-2′-phenylindole dihydrochloride (DAPI) to visualize nuclear.

Caco2-BBE cells grown on filters were washed and fixed with 4% paraformaldehyde in PBS with calcium for 20 min. The cells were then permeabilized with 0.1% Triton/PBS for 30 min at room temperature. Monolayers were incubated with rabbit SPAK antibody and then with relevant fluoresceinated secondary antibody same as for colon cryostat sections. Subsequently, monolayers were stained with rhodamine/phalloidin (Molecular Probes, Carlsbad, CA) to visualize actin. Samples were mounted in *p*-phenylenediamine/glycerol (1:1) and analyzed by confocal microscopy (Zeiss dual-laser confocal microscope).

Real time PCR

total RNA from Caco2-BBE cells, mucosa of mouse colon tissue and patients biopsy specimens were extracted with TRIzol reagent (Invitrogen, Carlsbad, CA), reverse transcribed using the Thermoscript^{TM} RT-PCR System (Invitrogen, Carlsbad, CA) and purified with the RNeasy Mini Kit (Qiagen, Germantown, MD). Real time PCRs were performed using iQ SYBR Green Supermix kit (Bio-Rad, Hercules, CA) with the iCycler sequence detection system (Bio-Rad, Hercules, CA) with specific primers. For human SPAK: sense 5′ TGGAATTAGCAACAGGAGCAGCG 3′, antisense 5′ TTTCCAAAGTGGGTGGATCATTT 3′, GAPDH acts as internal control: sense 5′ ACCACAGTCCATGCCATCAC 3′, antisense 5′ TCCACCACCCTGTTGCTGTA 3′. For mouse SPAK: sense 5′ GTAAGGCGAGTTCCTGGGTCG 3′, antisense 5′ CCAGTCGCCGTCTTCAGTCTT 3′ 36B4 acts as internal control: sense 5′ TCCAGGCTTTGGGCATCA 3′, antisense 5′ CTTTATCAGCTGCACATCACTCAGA.

Nuclear protein extraction

Nuclear protein was extracted from Caco2-BBE cells or mucosa from mice colon tissue treated with hyperosmotic medium. Cells and mucosa were washed once in ice-cold PBS, and centrifuged at 800 rpm for 5 min. The resulting pellets were resuspended in 5 ml of cold lysis buffer (10 mM HEPES, 10 mM KC1, 1.5 mM $MgC1_2$, and 0.1% Nonidet P-40; pH 7.9 at 4°C) for 10 min on ice. For the isolation of nuclei, the lysate was vigorously mixed and centrifuged for 5 min at 12,000 *g* and 4°C, and the nuclear pellet was washed once with 1 ml of Nonidet P-40-free lysis buffer. For the extraction of nuclear proteins, the nuclear pellet was resuspended in 1 ml of protein extraction buffer (420 mM NaCl, 20 mM HEPES, 1.5 $MgCl_2$, 0.2 mM EDTA, and 25% glycerol; pH 7.9) for 10 min at 4°C. After being vigorous mixed, the nuclear suspension was centrifuged for 5 min at 4°C. The protein content in the final supernatant (nuclear protein extract) was measured using the Bradford method (Bio-Rad, Hercules, CA). DTT (0.5 mM), PMSF (0.5 mM), and leupeptin (10 pg/ml) were added to the lysis and extraction buffers just before use. The diluting buffer contained the same amounts of DTT and leupeptin but only 0.2 mM PMSF. Samples were stored at −70°C until use.

Transient transfection and luciferase reporter gene assay

Renilla (phRL-CMV, 5 ng) and relevant SPAK promoter constructs (4 μg) were co-transfected into Caco2-BBE cells with Lipofectin (Invitrogen, Carlsbad, CA). After stimulation, the resulting luminescence was measured for 10 s in a luminometer (Luminoskan, Thermal Labsystems, MA). Each luciferase activity was normalized based on the control Renilla luciferase activity.

Extracts were analyzed in triplicate, and each experiment was performed for at least three times.

Electrophoretic Mobility Shift Assays (EMSAs)

Probes were end labeled with a Biotin 3′ End DNA Labeling Kit (Pierce, Rockford, IL). Standard EMSAs and supershift EMSAs with relevant antibodies were performed using the LightShift Chemiluminescent EMSA Kit (Pierce, Rockford, IL). Probe labeling and protocol for EMSAs were as described previously [29].

Chromatin immunoprecipitation assay

Sp1 and NF-κB chromatin immunoprecipitation (ChIP) assays of Caco2-BBE cells treated with hyperosmolarity (610 mOsm) for 30 min were performed using the ChIP Assay Kit (Upstate Cell Signaling Solutions, Lake Placid, NY) according to the manufacturer's instructions. Briefly, Caco2-BBE cells were fixed with 1% formaldehyde for 10 minutes at 37°C to initiate cross-linking, scraped off the plate, washed with ice-cold PBS, and resuspended in 200 μl of sodium dodecyl sulfate lysis buffer for 10 minutes on ice. Cells were then sonicated with three sets of 10-second pulses at 35% power to shear the DNA into 200 1,000-bp fragments. Samples were centrifuged, and the supernatant (used as total DNA input) was diluted in ChIP dilution buffer and precleared with a protein A agarose-salmon sperm DNA slurry to reduce the nonspecific background. Samples were then immunoprecipitated with 2 μg of mouse anti-Sp1 (Upstate Cell Signaling Solutions) or 3 μg of rabbit anti-p65 antibody (Santa Cruz Biotechnology) overnight at 4°C. Complexes were collected in a protein A agarose-salmon sperm DNA slurry for 1 hour at 4°C, washed once each with the provided low-salt, high-salt, and LiCl wash buffers, and then washed twice in Tris-EDTA buffer [10 mmol/L Tris-HCl (pH 8.0) and 1 mmol/L EDTA]. The immunoprecipitated chromatin was eluted from protein A using freshly prepared elution buffer (100 mmol/L $NaHCO_3$ and 1% sodium dodecyl sulfate), and the protein-DNA cross-links were reversed by treatment with NaCl (200 mmol/L) at 65°C for 4 hours. The DNA was purified by incubation with proteinase K at 45°C for 1 hour, followed by phenol-chloroform extraction and ethanol precipitation with glycogen. Sp1 (I, II, and III) and NF-κB binding sites in immunoprecipitates were detected by PCR using the following specific primers: Sp1 IF 5′ GTAAATGAACTTCAGGTTCTCTTTG 3′, Sp1 IR: 5′ CGCCCTGCGCCTTGGCCC CAGACGA 3′; Sp1 IIF 5′ AGCACACACAAAGCGGCCTGACTCC 3′, Sp1 IIR 5′ CCCAGAGCCTAGCGCGCGCTGTTCT 3′; Sp1 IIIF 5′ CTGGCTTCGGCGGGGAC GGCGGCGG 3′; Sp1 IIIR 5′ CCATGATGCTGCGGAGGAGAGCAGGAG 3′; NF-κBF 5′ GGCGCAGGGCGAGCAGGGAGGGAGG 3′, NF-κBR 5′ TGTTCTCCGCCTCGG CGAGGGGAAC 3′. The products were resolved on a 1% agarose gel and visualized with ethidium bromide.

Transfection of siRNA

Subconfluent (60%) Caco2-BBE cells plated on six-well plates (Costar, Corning, NY) were transfected with siRNA duplexes directed against Sp1 and NF-κB, and a non targeting siRNA was used as the control for non-sequence-specific effects of siRNAs (Ambion, Austin, TX) using Lipofectamine 2000 (Invitrogen, Carlsbad, CA) in serum-free medium. Serum was added after 24 h, Caco2-BBE cells underwent hyperosmolarity treatment (610 mOsm) for 30 min; cells were then collected for western blot analysis with relevant antibodies.

Nuclear run-on assay

Nuclear run-on assay was performed following the previous protocol [94] with little modification. Briefly; nuclei were isolated from Caco2-BBE cells treated with or without hyperosmolarity for 1 hour. Around 5×10^7 cells were pelleted then lysed on ice for 10 min in lysis buffer containing 0.3 M sucrose, 0.4% (v/v) NP-40, 10 mM Tris-HCl at pH 7.4, 10 mM NaCl, and 3 mM $MgCl_2$. After centrifugation (15 min at 500 relative centrifuge force), the nuclear pellet was resuspended and subjected to a repeat (5 min) lysis to remove any remaining intact cells. Following centrifugation, nuclei were purified by centrifugation through a 2.0 M sucrose cushion. The nuclei were resuspended in 300 μl of transcription buffer (50 mM Tris-HCl [pH 8.0], 150 mM KCl, 5 mM $MgCl_2$, 0.5 mM $MnCl_2$, 1 mM dithiothreitol, 0.1 mM EDTA, 10% glycerol). After pretreatment with 1 μl of 50 μg/ml RNase A and followed by 2.5 μl of 100 units RNasin, the *in vitro* elongation reaction was initiated with the addition of ribonucleotides to a final concentration of 0.25 mM each ATP, GTP, CTP and UTP. The reaction was carried out for 25 min at 30°C. After incubation with RNase-free DNase, RNA was extracted with phenol-chloroform, precipitated with ammonium acetate and isopropanol, washed with 70% ethanol, and dissolved in water. cDNA was synthesized with The SuperScript® III First-Strand Synthesis System (Invitrogen, Carlsbad, CA) and amplified with Platinum Taq DNA polymerase (Invitrogen, Carlsbad, CA) using SPAK HQF and SPAK HQR as primers. GAPDH acts as internal control. The products were resolved on a 1.5% agarose gel and visualized with ethidium bromide.

SPAK mRNA stability assay and northern blot

For mRNA decay experiments, Caco2-BBE cells pretreated with actinomycin D (5 μg/ml) for 1 hour to arrest transcription were cultured in hyperosmotic medium (610 mOsm) or isoosmotic DMEM at indicated time points. The decay of SPAK mRNA was examined by real time PCR with specific primers SPAKHQF: 5′ TGGAATTAGCAACAGGAGCAGCG 3′ and SPAKHQR: 5′ TTTCCAAAGTGGGTGGATCATTT 3′. Levels of mRNA were then standardized against 18s rRNA levels with primers 18SF: 5′ CCCCTCGATGCTCTTAGCTGAGTGT 3′ and 18SR: 5′ CGCCGGTCCAAGAATTTCACCTCT 3′, taking into account a previous determination of 65 hours for 18s rRNA half life [95], and plotted as the percentage of remaining mRNA compared to message levels at the 0 time point (where there is a 100% maximum mRNA level). The 1-hour time point sample was also used for Northern blot analysis with the North2South complete biotin random prime labeling and detection kit (Pierce, Rockford, IL) with probe generated by PCR with primers: SPAKNorFor 5′ CTGATTGAGAAGCTGCTTACAAG 3′ and SPAKNorRev 5′ CAAGAAGAAGCTTCTCTGTAGTC 3′.

Permeability assay

In vitro and *in vivo* permeability assays to determine barrier function were performed using the FITC-Dextran method as described previously [96,97]. For *in vito* permeability assays, Caco2-BBE cells transfected with SPAK/pcDNA6, vector pcDNA6, SPAK siRNA (Ambion, Austin, TX) and con siRNA (same sequence with random order) were plated on transwell filters (Costar, Corning, New York) to grow to just confluency. For permeability assays, 100 μl of conditioned medium with FITC-Dextran (10 mg/ml, MW 4 kDa; Sigma-Aldrich, ST. Louis, MO) are added into the upper chamber of the transwell chamber, the plate is incubated at 37°C in an atmosphere of 5% CO_2. Samples are taken from the lower chamber with/without treatment of hyperosmolarity (610 mOsm) for 30 min. The permeability of the

epithelial monolayer correlates with the fluorescence intensity in the lower chamber (λ ex = 492 nm, λ em = 510 nm; Cytofluor 2300; Millipore, Waters Chromatography). Values are shown as nanograms per milliliter per minute FITC-dextran present in the basolateral reservoir. For *in vivo* permeability assay, 8-wk old wild type and SPAK transgenic mice were used. Food and water were withdrawn for 4 h and mice were gavaged with permeability tracer FITC-labeled dextran (60 mg/100 g body weight MW 4 kDa; Sigma-Aldrich, ST. Louis, MO). Serum was collected retro-orbitally 4 h after gavage; fluorescence intensity of each sample was measured (λ ex = 492 nm, λ em = 510 nm; Cytofluor 2300; Millipore, Waters Chromatography); and FITC-dextran concentrations were determined from standard curves generated by serial dilution of FITC-dextran and represented as μg FITC-dextran/μg protein.

Supporting Information

Figure S1

Found at: doi:10.1371/journal.pone.0005049.s001 (0.65 MB DOC)

Figure S2

Found at: doi:10.1371/journal.pone.0005049.s002 (0.03 MB DOC)

Figure S3

Found at: doi:10.1371/journal.pone.0005049.s003 (0.27 MB DOC)

Author Contributions

Conceived and designed the experiments: YY SVS DM. Performed the experiments: YY GD. Analyzed the data: YY GD HTTN TSO DM. Contributed reagents/materials/analysis tools: YY GD HTTN TSO DM. Wrote the paper: YY DM.

References

1. Schilli R, Breuer RI, Klein F, Dunn K, Gnaedinger A, et al. (1982) Comparison of the composition of faecal fluid in Crohn's disease and ulcerative colitis. Gut 23: 326–332.
2. Katz KD, Hollander D, Vadheim CM, McElree C, Delahunty T, et al. (1989) Intestinal permeability in patients with Crohn's disease and their healthy relatives. Gastroenterology 97: 927–931.
3. Sandle GI, Higgs N, Crowe P, Marsh MN, Venkatesan S, et al. (1990) Cellular basis for defective electrolyte transport in inflamed human colon. Gastroenterology 99: 97–105.
4. Vernia P, Gnaedinger A, Hauck W, Breuer RI (1988) Organic anions and the diarrhea of inflammatory bowel disease. Dig Dis Sci 33: 1353–1358.
5. Cheromcha DP, Hyman PE (1988) Neonatal necrotizing enterocolitis. Inflammatory bowel disease of the newborn. Dig Dis Sci 33: 78S–84S.
6. Li DQ, Chen Z, Song XJ, Luo L, Pflugfelder SC (2004) Stimulation of matrix metalloproteinases by hyperosmolarity via a JNK pathway in human corneal epithelial cells. Invest Ophthalmol Vis Sci 45: 4302–4311.
7. Shapiro L, Dinarello CA (1997) Hyperosmotic stress as a stimulant for proinflammatory cytokine production. Exp Cell Res 231: 354–362.
8. Hashimoto S, Matsumoto K, Gon Y, Nakayama T, Takeshita I, et al. (1999) Hyperosmolarity-induced interleukin-8 expression in human bronchial epithelial cells through p38 mitogen-activated protein kinase. Am J Respir Crit Care Med 159: 634–640.
9. Loitsch SM, von Mallinckrodt C, Kippenberger S, Steinhilber D, Wagner TO, et al. (2000) Reactive oxygen intermediates are involved in IL-8 production induced by hyperosmotic stress in human bronchial epithelial cells. Biochem Biophys Res Commun 276: 571–578.
10. Nemeth ZH, Deitch EA, Szabo C, Hasko G (2002) Hyperosmotic stress induces nuclear factor-kappaB activation and interleukin-8 production in human intestinal epithelial cells. Am J Pathol 161: 987–996.
11. Asakawa H, Miyagawa J, Hanafusa T, Kuwajima M, Matsuzawa Y (1997) High glucose and hyperosmolarity increase secretion of interleukin-1 beta in cultured human aortic endothelial cells. J Diabetes Complications 11: 176–179.
12. Hubert A, Cauliez B, Chedeville A, Husson A, Lavoinne A (2004) Osmotic stress, a proinflammatory signal in Caco-2 cells. Biochimie 86: 533–541.
13. Li DQ, Luo L, Chen Z, Kim HS, Song XJ, et al. (2006) JNK and ERK MAP kinases mediate induction of IL-1beta, TNF-alpha and IL-8 following hyperosmolar stress in human limbal epithelial cells. Exp Eye Res 82: 588–596.
14. Ochi H, Masuda J, Gimbrone MA (2002) Hyperosmotic stimuli inhibit VCAM-1 expression in cultured endothelial cells via effects on interferon regulatory factor-1 expression and activity. Eur J Immunol 32: 1821–1831.
15. Abolhassani M, Wertz X, Pooya M, Chaumet-Riffaud P, Guais A, et al. (2008) Hyperosmolarity causes inflammation through the methylation of protein phosphatase 2A. Inflamm Res.
16. Luo L, Li DQ, Corrales RM, Pflugfelder SC (2005) Hyperosmolar saline is a proinflammatory stress on the mouse ocular surface. Eye Contact Lens 31: 186–193.
17. Katsuyama I, Arakawa T (2003) A convenient rabbit model of ocular epithelium damage induced by osmotic dehydration. J Ocul Pharmacol Ther 19: 281–289.
18. Bagrodia S, Cerione RA (1999) Pak to the future. Trends Cell Biol 9: 350–355.
19. Kyriakis JM (1999) Signaling by the germinal center kinase family of protein kinases. J Biol Chem 274: 5259–5262.
20. Widmann C, Gibson S, Jarpe MB, Johnson GL (1999) Mitogen-activated protein kinase: conservation of a three-kinase module from yeast to human. Physiol Rev 79: 143–180.
21. Ip YT, Davis RJ (1998) Signal transduction by the c-Jun N-terminal kinase (JNK)–from inflammation to development. Curr Opin Cell Biol 10: 205–219.
22. Klipp E, Nordlander B, Kruger R, Gennemark P, Hohmann S (2005) Integrative model of the response of yeast to osmotic shock. Nat Biotechnol 23: 975–982.
23. Endo J, Toyama-Sorimachi N, Taya C, Kuramochi-Miyagawa S, Nagata K, et al. (2000) Deficiency of a STE20/PAK family kinase LOK leads to the acceleration of LFA-1 clustering and cell adhesion of activated lymphocytes. FEBS Lett 468: 234–238.
24. Wagner S, Flood TA, O'Reilly P, Hume K, Sabourin LA (2002) Association of the Ste20-like kinase (SLK) with the microtubule. Role in Rac1-mediated regulation of actin dynamics during cell adhesion and spreading. J Biol Chem 277: 37685–37692.
25. Stockton RA, Schaefer E, Schwartz MA (2004) p21-activated kinase regulates endothelial permeability through modulation of contractility. J Biol Chem 279: 46621–46630.
26. Stockton R, Reutershan J, Scott D, Sanders J, Ley K, et al. (2007) Induction of vascular permeability: beta PIX and GIT1 scaffold the activation of extracellular signal-regulated kinase by PAK. Mol Biol Cell 18: 2346–2355.
27. Johnston AM, Naselli G, Gonez LJ, Martin RM, Harrison LC, et al. (2000) SPAK, a STE20/SPS1-related kinase that activates the p38 pathway. Oncogene 19: 4290–4297.
28. Yan Y, Nguyen H, Dalmasso G, Sitaraman SV, Merlin D (2007) Cloning and characterization of a new intestinal inflammation-associated colonic epithelial Ste20-related protein kinase isoform. Biochim Biophys Acta 1769: 106–116.
29. Yan Y, Dalmasso G, Nguyen HT, Obertone TS, Charrier-Hisamuddin L, et al. (2008) Nuclear factor-kappaB is a critical mediator of Ste20-like proline-/alanine-rich kinase regulation in intestinal inflammation. Am J Pathol 173: 1013–1028.
30. Dan I, Watanabe NM, Kusumi A (2001) The Ste20 group kinases as regulators of MAP kinase cascades. Trends Cell Biol 11: 220–230.
31. Li Y, Hu J, Vita R, Sun B, Tabata H, et al. (2004) SPAK kinase is a substrate and target of PKCtheta in T-cell receptor-induced AP-1 activation pathway. Embo J 23: 1112–1122.
32. Piechotta K, Lu J, Delpire E (2002) Cation chloride cotransporters interact with the stress-related kinases Ste20-related proline-alanine-rich kinase (SPAK) and oxidative stress response 1 (OSR1). J Biol Chem 277: 50812–50819.
33. Dowd BF, Forbush B (2003) PASK (proline-alanine-rich STE20-related kinase), a regulatory kinase of the Na-K-Cl cotransporter (NKCC1). J Biol Chem 278: 27347–27353.
34. Gagnon KB, England R, Delpire E (2006) Characterization of SPAK and OSR1, regulatory kinases of the Na-K-2Cl cotransporter. Mol Cell Biol 26: 689–698.
35. Topper JN, Wasserman SM, Anderson KR, Cai J, Falb D, et al. (1997) Expression of the bumetanide-sensitive Na-K-Cl cotransporter BSC2 is differentially regulated by fluid mechanical and inflammatory cytokine stimuli in vascular endothelium. J Clin Invest 99: 2941–2949.
36. Nguyen M, Pace AJ, Koller BH (2007) Mice lacking NKCC1 are protected from development of bacteremia and hypothermic sepsis secondary to bacterial pneumonia. J Exp Med 204: 1383–1393.
37. Gamba G (2005) Molecular physiology and pathophysiology of electroneutral cation-chloride cotransporters. Physiol Rev 85: 423–493.
38. Hallows KR, Law FY, Packman CH, Knauf PA (1996) Changes in cytoskeletal actin content, F-actin distribution, and surface morphology during HL-60 cell volume regulation. J Cell Physiol 167: 60–71.
39. Rizoli SB, Rotstein OD, Parodo J, Phillips MJ, Kapus A (2000) Hypertonic inhibition of exocytosis in neutrophils: central role for osmotic actin skeleton remodeling. Am J Physiol Cell Physiol 279: C619–633.

40. Pinto D, Robine S, Jaisser F, El Marjou FE, Louvard D (1999) Regulatory sequences of the mouse villin gene that efficiently drive transgenic expression in immature and differentiated epithelial cells of small and large intestines. J Biol Chem 274: 6476–6482.
41. Hirayama T, Maeda T, Saito H, Shinozaki K (1995) Cloning and characterization of seven cDNAs for hyperosmolarity-responsive (HOR) genes of Saccharomyces cerevisiae. Mol Gen Genet 249: 127–138.
42. El-Sherbeny A, Naggar H, Miyauchi S, Ola MS, Maddox DM, et al. (2004) Osmoregulation of taurine transporter function and expression in retinal pigment epithelial, ganglion, and muller cells. Invest Ophthalmol Vis Sci 45: 694–701.
43. Baudouin-Legros M, Brouillard F, Cougnon M, Tondelier D, Leclerc T, et al. (2000) Modulation of CFTR gene expression in HT-29 cells by extracellular hyperosmolarity. Am J Physiol Cell Physiol 278: C49–56.
44. Briggs MR, Kadonaga JT, Bell SP, Tjian R (1986) Purification and biochemical characterization of the promoter-specific transcription factor, Sp1. Science 234: 47–52.
45. Saffer JD, Jackson SP, Annarella MB (1991) Developmental expression of Sp1 in the mouse. Mol Cell Biol 11: 2189–2199.
46. Jones KA, Kadonaga JT, Luciw PA, Tjian R (1986) Activation of the AIDS retrovirus promoter by the cellular transcription factor, Sp1. Science 232: 755–759.
47. Hayden MS, Ghosh S (2004) Signaling to NF-kappaB. Genes Dev 18: 2195–2224.
48. Hoffmann A, Baltimore D (2006) Circuitry of nuclear factor kappaB signaling. Immunol Rev 210: 171–186.
49. Kunsch C, Rosen CA (1993) NF-kappa B subunit-specific regulation of the interleukin-8 promoter. Mol Cell Biol 13: 6137–6146.
50. Ghosh S, May MJ, Kopp EB (1998) NF-kappa B and Rel proteins: evolutionarily conserved mediators of immune responses. Annu Rev Immunol 16: 225–260.
51. Zhang G, Ghosh S (2001) Toll-like receptor-mediated NF-kappaB activation: a phylogenetically conserved paradigm in innate immunity. J Clin Invest 107: 13–19.
52. Scheinman RI, Cogswell PC, Lofquist AK, Baldwin AS Jr (1995) Role of transcriptional activation of I kappa B alpha in mediation of immunosuppression by glucocorticoids. Science 270: 283–286.
53. Visekruna A, Joeris T, Seidel D, Kroesen A, Loddenkemper C, et al. (2006) Proteasome-mediated degradation of IkappaBalpha and processing of p105 in Crohn disease and ulcerative colitis. J Clin Invest 116: 3195–3203.
54. Perkins ND, Edwards NL, Duckett CS, Agranoff AB, Schmid RM, et al. (1993) A cooperative interaction between NF-kappa B and Sp1 is required for HIV-1 enhancer activation. Embo J 12: 3551–3558.
55. Gomez-Gonzalo M, Carretero M, Rullas J, Lara-Pezzi E, Aramburu J, et al. (2001) The hepatitis B virus X protein induces HIV-1 replication and transcription in synergy with T-cell activation signals: functional roles of NF-kappaB/NF-AT and SP1-binding sites in the HIV-1 long terminal repeat promoter. J Biol Chem 276: 35435–35443.
56. Sheppard KA, Rose DW, Haque ZK, Kurokawa R, McInerney E, et al. (1999) Transcriptional activation by NF-kappaB requires multiple coactivators. Mol Cell Biol 19: 6367–6378.
57. Kerr LD, Ransone LJ, Wamsley P, Schmitt MJ, Boyer TG, et al. (1993) Association between proto-oncoprotein Rel and TATA-binding protein mediates transcriptional activation by NF-kappa B. Nature 365: 412–419.
58. Shu HB, Agranoff AB, Nabel EG, Leung K, Duckett CS, et al. (1993) Differential regulation of vascular cell adhesion molecule 1 gene expression by specific NF-kappa B subunits in endothelial and epithelial cells. Mol Cell Biol 13: 6283–6289.
59. Neish AS, Read MA, Thanos D, Pine R, Maniatis T, et al. (1995) Endothelial interferon regulatory factor 1 cooperates with NF-kappa B as a transcriptional activator of vascular cell adhesion molecule 1. Mol Cell Biol 15: 2558–2569.
60. Sanceau J, Kaisho T, Hirano T, Wietzerbin J (1995) Triggering of the human interleukin-6 gene by interferon-gamma and tumor necrosis factor-alpha in monocytic cells involves cooperation between interferon regulatory factor-1, NF kappa B, and Sp1 transcription factors. J Biol Chem 270: 27920–27931.
61. Hirano F, Tanaka H, Hirano Y, Hiramoto M, Handa H, et al. (1998) Functional interference of Sp1 and NF-kappaB through the same DNA binding site. Mol Cell Biol 18: 1266–1274.
62. Lang KS, Weigert C, Braedel S, Fillon S, Palmada M, et al. (2003) Inhibition of interferon-gamma expression by osmotic shrinkage of peripheral blood lymphocytes. Am J Physiol Cell Physiol 284: C200–208.
63. Hao CM, Yull F, Blackwell T, Komhoff M, Davis LS, et al. (2000) Dehydration activates an NF-kappaB-driven, COX2-dependent survival mechanism in renal medullary interstitial cells. J Clin Invest 106: 973–982.
64. Auphan N, DiDonato JA, Rosette C, Helmberg A, Karin M (1995) Immunosuppression by glucocorticoids: inhibition of NF-kappa B activity through induction of I kappa B synthesis. Science 270: 286–290.
65. Lenardo MJ, Baltimore D (1989) NF-kappa B: a pleiotropic mediator of inducible and tissue-specific gene control. Cell 58: 227–229.
66. Lenardo MJ, Fan CM, Maniatis T, Baltimore D (1989) The involvement of NF-kappa B in beta-interferon gene regulation reveals its role as widely inducible mediator of signal transduction. Cell 57: 287–294.
67. Kopp E, Ghosh S (1994) Inhibition of NF-kappa B by sodium salicylate and aspirin. Science 265: 956–959.
68. So WV, Rosbash M (1997) Post-transcriptional regulation contributes to Drosophila clock gene mRNA cycling. Embo J 16: 7146–7155.
69. Carter AB, Monick MM, Hunninghake GW (1999) Both Erk and p38 kinases are necessary for cytokine gene transcription. Am J Respir Cell Mol Biol 20: 751–758.
70. Bagnasco SM, Murphy HR, Bedford JJ, Burg MB (1988) Osmoregulation by slow changes in aldose reductase and rapid changes in sorbitol flux. Am J Physiol 254: C788–792.
71. Moriyama T, Garcia-Perez A, Burg MB (1989) Osmotic regulation of aldose reductase protein synthesis in renal medullary cells. J Biol Chem 264: 16810–16814.
72. Schweigel M, Freyer M, Leclercq S, Etschmann B, Lodemann U, et al. (2005) Luminal hyperosmolarity decreases Na transport and impairs barrier function of sheep rumen epithelium. J Comp Physiol [B] 175: 575–591.
73. Safdar Z, Wang P, Ichimura H, Issekutz AC, Quadri S, et al. (2003) Hyperosmolarity enhances the lung capillary barrier. J Clin Invest 112: 1541–1549.
74. Han J, Lee JD, Bibbs L, Ulevitch RJ (1994) A MAP kinase targeted by endotoxin and hyperosmolarity in mammalian cells. Science 265: 808–811.
75. Luo L, Li DQ, Pflugfelder SC (2007) Hyperosmolarity-induced apoptosis in human corneal epithelial cells is mediated by cytochrome c and MAPK pathways. Cornea 26: 452–460.
76. Bruewer M, Luegering A, Kucharzik T, Parkos CA, Madara JL, et al. (2003) Proinflammatory cytokines disrupt epithelial barrier function by apoptosis-independent mechanisms. J Immunol 171: 6164–6172.
77. Mosser DD, Caron AW, Bourget L, Denis-Larose C, Massie B (1997) Role of the human heat shock protein hsp70 in protection against stress-induced apoptosis. Mol Cell Biol 17: 5317–5327.
78. Yujiri T, Sather S, Fanger GR, Johnson GL (1998) Role of MEKK1 in cell survival and activation of JNK and ERK pathways defined by targeted gene disruption. Science 282: 1911–1914.
79. Duzgun SA, Rasque H, Kito H, Azuma N, Li W, et al. (2000) Mitogen-activated protein phosphorylation in endothelial cells exposed to hyperosmolar conditions. J Cell Biochem 76: 567–571.
80. Galvez AS, Ulloa JA, Chiong M, Criollo A, Eisner V, et al. (2003) Aldose reductase induced by hyperosmotic stress mediates cardiomyocyte apoptosis: differential effects of sorbitol and mannitol. J Biol Chem 278: 38484–38494.
81. Howe KL, Reardon C, Wang A, Nazli A, McKay DM (2005) Transforming growth factor-beta regulation of epithelial tight junction proteins enhances barrier function and blocks enterohemorrhagic Escherichia coli O157:H7-induced increased permeability. Am J Pathol 167: 1587–1597.
82. Dudek SM, Garcia JG (2001) Cytoskeletal regulation of pulmonary vascular permeability. J Appl Physiol 91: 1487–1500.
83. Shasby DM, Shasby SS, Sullivan JM, Peach MJ (1982) Role of endothelial cell cytoskeleton in control of endothelial permeability. Circ Res 51: 657–661.
84. Poli A, Coleman PJ, Mason RM, Levick JR (2002) Contribution of F-actin to barrier properties of the blood-joint pathway. Microcirculation 9: 419–430.
85. Omori K, Shikata Y, Sarai K, Watanabe N, Wada J, et al. (2007) Edaravone mimics sphingosine-1-phosphate-induced endothelial barrier enhancement in human microvascular endothelial cells. Am J Physiol Cell Physiol 293: C1523–1531.
86. Ilic D, Mao-Qiang M, Crumrine D, Dolganov G, Larocque N, et al. (2007) Focal adhesion kinase controls pH-dependent epidermal barrier homeostasis by regulating actin-directed Na+/H+ exchanger 1 plasma membrane localization. Am J Pathol 170: 2055–2067.
87. Goyette P, Labbe C, Trinh TT, Xavier RJ, Rioux JD (2007) Molecular pathogenesis of inflammatory bowel disease: genotypes, phenotypes and personalized medicine. Ann Med 39: 177–199.
88. Dignass AU, Baumgart DC, Sturm A (2004) Review article: the aetiopathogenesis of inflammatory bowel disease–immunology and repair mechanisms. Aliment Pharmacol Ther 20 Suppl 4: 9–17.
89. Clayburgh DR, Shen L, Turner JR (2004) A porous defense: the leaky epithelial barrier in intestinal disease. Lab Invest 84: 282–291.
90. Craxton A, Shu G, Graves JD, Saklatvala J, Krebs EG, et al. (1998) p38 MAPK is required for CD40-induced gene expression and proliferation in B lymphocytes. J Immunol 161: 3225–3236.
91. Hollenbach E, Neumann M, Vieth M, Roessner A, Malfertheiner P, et al. (2004) Inhibition of p38 MAP kinase- and RICK/NF-kappaB-signaling suppresses inflammatory bowel disease. Faseb J 18: 1550–1552.
92. Zenzie-Gregory B, Khachi A, Garraway IP, Smale ST (1993) Mechanism of initiator-mediated transcription: evidence for a functional interaction between the TATA-binding protein and DNA in the absence of a specific recognition sequence. Mol Cell Biol 13: 3841–3849.
93. Zhang DE, Hetherington CJ, Tan S, Dziennis SE, Gonzalez DA, et al. (1994) Sp1 is a critical factor for the monocytic specific expression of human CD14. J Biol Chem 269: 11425–11434.
94. Gnoni GV, Geelen MJ, Bijleveld C, Quagliariello E, van den Bergh SG (1985) Short-term stimulation of lipogenesis by triiodothyronine in maintenance cultures of rat hepatocytes. Biochem Biophys Res Commun 128: 525–530.
95. Nwagwu M, Nana M (1980) Ribonucleic acid synthesis in embryonic chick muscle, rates of synthesis and half-lives of transfer and ribosomal RNA species. J Embryol Exp Morphol 56: 253–267.

96. Furuta GT, Turner JR, Taylor CT, Hershberg RM, Comerford K, et al. (2001) Hypoxia-inducible factor 1-dependent induction of intestinal trefoil factor protects barrier function during hypoxia. J Exp Med 193: 1027–1034.

97. Garg P, Rojas M, Ravi A, Bockbrader K, Epstein S, et al. (2006) Selective ablation of matrix metalloproteinase-2 exacerbates experimental colitis: contrasting role of gelatinases in the pathogenesis of colitis. J Immunol 177: 4103–4112.